ORIGINAL ARTICLE

Reducing the draconitic errors in GNSS geodetic products

**C. J. Rodriguez-Solano · U. Hugentobler ·
P. Steigenberger · M. Bloßfeld · M. Fritsche**

Abstract Systematic errors at harmonics of the GPS draconitic year have been found in diverse GPS-derived geodetic products like the geocenter Z-component, station coordinates, Y-pole rate and orbits (i.e. orbit overlaps). The GPS draconitic year is the repeat period of the GPS constellation w.r.t. the Sun which is about 351 days. Different error sources have been proposed which could generate these spurious signals at the draconitic harmonics. In this study, we focus on one of these error sources, namely the radiation pressure orbit modeling deficiencies. For this purpose, three GPS+GLONASS solutions of 8 years (2004–2011) were computed which differ only in the solar radiation pressure (SRP) and satellite attitude models. The models employed in the solutions are: (1) the CODE (5-parameter) radiation pressure model widely used within the International GNSS Service community, (2) the adjustable box-wing model for SRP impacting GPS (and GLONASS) satellites, and (3) the adjustable box-wing model upgraded to use non-nominal yaw attitude, specially for satellites in eclipse seasons. When comparing the first solution with the third one we achieved the following in the GNSS geodetic products. Orbits: the draconitic errors in the orbit overlaps are reduced for the GPS satellites in all the harmonics on average 46, 38 and 57 % for the radial, along-track and cross-track components, while for GLONASS satellites they are mainly reduced in the cross-track component by 39 %. Geocenter Z-component: all

C. J. Rodriguez-Solano (✉) · U. Hugentobler · P. Steigenberger
Institut für Astronomische und Physikalische Geodäsie, Technische
Universität München, 80333 Munich, Germany
e-mail: rodriguez@bv.tum.de

M. Bloßfeld
Deutsches Geodätisches Forschungsinstitut, 80539 Munich, Germany

M. Fritsche
Institut für Planetare Geodäsie, Technische Universität Dresden,
01069 Dresden, Germany

the odd draconitic harmonics found when the CODE model is used show a very important reduction (almost disappearing with a 92 % average reduction) with the new radiation pressure models. Earth orientation parameters: the draconitic errors are reduced for the X-pole rate and especially for the Y-pole rate by 24 and 50 % respectively. Station coordinates: all the draconitic harmonics (except the 2nd harmonic in the North component) are reduced in the North, East and Height components, with average reductions of 41, 39 and 35 % respectively. This shows, that part of the draconitic errors currently found in GNSS geodetic products are definitely induced by the CODE radiation pressure orbit modeling deficiencies.

1 Introduction

Systematic errors at harmonics of the GPS draconitic year have been found in diverse GPS-derived geodetic products. The GPS draconitic year is the repeat period of the GPS constellation w.r.t. the Sun, which is about 351 days or 1.04 cpy (cycles per year). This period results from the secular retrograde motion of the right ascension of the ascending node due to the oblateness of the Earth (i.e. due to the J2 term). The GPS-derived geodetic products in which spurious signals have been found at 1.04 cpy and its harmonics are the following:

– Geocenter Z-component (Hugentobler et al. 2006; Meindl 2011; Rodriguez-Solano et al. 2012a; Ostini 2012).
– Station coordinates (Ray et al. 2008; Collilieux et al. 2007; Amiri-Simkooei 2007; Tregoning and Watson

2009; King and Watson 2010; Santamaría-Gómez et al. 2011; Rodriguez-Solano et al. 2012a; Ostini 2012).
- Y-pole rate (Seitz et al. 2012).
- Orbits (jumps between successive days, Griffiths and Ray 2013).

For other GNSS constellations similar systematic errors could be expected at harmonics of the respective draconitic years, e.g., for GLONASS the draconitic year is about 353 days or 1.035 cpy. Meindl (2011) found odd harmonics of the GLONASS draconitic year in the time series of the Z-component of the GLONASS-only derived geocenter. For combined GPS+GLONASS products (like the ones generated in this study) the system-specific systematic errors are difficult to distinguish from the low harmonics of the draconitic years, as the fundamental frequencies are very close to each other. In the case of other space techniques such as DORIS, Gobinddass et al. (2009) found artifacts in the derived geocenter Z-component and station coordinates related to errors in the solar radiation pressure modeling (for TOPEX/Poseidon, SPOTs, ENVISAT and Jason-1 satellites).

Systematic errors in the GNSS data or models are expected to propagate over the whole GNSS solutions introducing these artificial effects on most products. Diverse error sources have been proposed to explain these systematic errors. Hugentobler et al. (2006) and Meindl et al. (2013) relate the geocenter motion with the orbit modeling parameters, in particular radiation pressure parameters, due to correlations between them. The first paper states that the patterns found in the geocenter Z-component with distinct periods of one GPS draconitic year should be caused by orbit modeling deficiencies and not by geophysical effects. Rebischung et al. (2014) found that the geocenter coordinates are highly collinear with the satellite clock and troposphere parameters, so that their estimation is very sensitive to GNSS modeling errors, like radiation pressure modeling errors. Ray et al. (2008) give two possible coupling mechanisms which could generate the spurious signals at harmonics of 1.04 cpy found in the estimates of station coordinates: (1) Long-period GPS satellite orbit modeling errors, in particular due to the Sun-satellite interactions or during eclipse seasons which happen twice per draconitic year for each orbital plane. (2) Station specific errors that can be aliased due to the repeating geometry of the satellite constellation w.r.t. the tracking network to generate a period of one draconitic year, in particular long-wavelength (i.e. near-field) multipath or errors in the antenna or radome calibrations. King and Watson (2010) demonstrated by using simulated GPS data that multipath errors can produce spurious signals at harmonics of 1.04 cpy on station coordinates time series. Tregoning and Watson (2009) and King and Watson (2010) found that if phase ambiguities are not fixed there is a significant amplification in the expression of the spurious draconitic harmonics. Tregoning and Watson (2009) and

Tregoning and Watson (2011) suggest that possible errors in the S1 and S2 tidal models (ocean, atmosphere) which are at diurnal and semidiurnal periods can contribute to the low-frequency draconitic signals seen in the GPS solutions. Griffiths and Ray (2013) introduced errors in the IERS (International Earth Rotation and Reference Systems Service) sub-daily Earth Orientation Parameters (EOP) tide model, which is used as a priori information in the GNSS solutions, and found that those errors can propagate to the GPS orbits at the 1st and 3rd harmonics of 1.04 cpy. Finally, Amiri-Simkooei (2013) focused on the nature of the draconitic errors found in GPS station coordinates and concluded that these errors do not likely depend on station related effects such as multipath but rather on other causes like orbit mismodeling or atmospheric loading effects.

In this study, we focus only on one of the error sources proposed by previous authors, namely the radiation pressure orbit modeling deficiencies. In Rodriguez-Solano et al. (2012a) we tested the impact of Earth radiation pressure on the draconitic errors present in station coordinates and geocenter Z-component, obtaining only a reduction (about 38 %) in the 6th harmonic of the North component of the station coordinates and just a minimal reduction for the harmonics of the geocenter Z-component. From that study it became clear that the modeling of the main non-conservative force acting on GPS satellites, the solar radiation pressure (SRP), should also be revised as we used the CODE radiation pressure model (Beutler et al. 1994). In Rodriguez-Solano et al. (2012b) we developed a new approach to model the SRP impacting GPS satellites which we called the adjustable box-wing model. This new model could reduce β_0 (Sun elevation angle above the orbital plane, see Fig. 1) dependent systematic errors observed in the orbit predictions of GPS-IIA, GPS-IIR and GLONASS-M satellites (Rodriguez-Solano et al. 2013). The β_0 angle varies with a period of one draconitic year, the maximum reachable values are given by the inclination of the satellite orbital plane plus the obliquity of the ecliptic (about 23.45°), i.e., $\pm 78.45°$ for GPS and $\pm 88.25°$ for GLONASS satellites. The reduction of β_0 systematic errors with the adjustable box-wing model only occurred outside eclipse seasons when the satellites are fully in nominal yaw attitude mode. During eclipse seasons when the satellites can perform yaw maneuvers the systematic errors were increased (especially for GPS-IIA satellites) with the adjustable box-wing model. Therefore, in Rodriguez-Solano et al. (2013) we upgraded the adjustable box-wing model to accommodate non-nominal yaw attitude, especially the yaw maneuvers performed during eclipse seasons, and with it obtaining an important reduction of the orbit errors during eclipse seasons for GPS-IIA satellites. This was an important motivation to start this study, with the reasoning that if we achieved a reduction of the β_0 systematic errors in the orbits, we will most probably also achieve a reduction of the orbit errors at
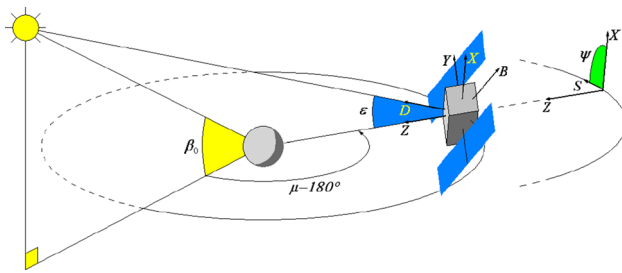
Fig. 1 Relative geometry of Sun, Earth and GPS satellites. Nominal yaw-steering attitude as a function of the position of the Sun in the orbital plane. Illustration of DYB (Sun-fixed) and XYZ (body-fixed) orthogonal frames

harmonics of the GPS draconitic year observed by Griffiths and Ray (2013). But we also suspected that the draconitic errors found in other GNSS derived geodetic products could be reduced since they were computed within the same GNSS solutions.

In a previous study by Sibthorpe et al. (2011), variants of the DYB model (Eq. (1), Beutler et al. 1994) were compared against the GPS Solar Pressure Model (GSPM) of Bar-Sever and Kuang (2004). The comparison between models was done by means of various internal (GIPSY-OASIS Software) and external metrics. The metrics supporting the use of the GSPM approach are: ambiguity resolution statistics, orbit overlaps, SLR tracking residuals, station repeatabilities, and GRACE K-band ranging statistics. However, clock overlaps between consecutive days and LOD (Length of Day) differences to IERS Bulletin A seem to favor the DYB approach.

The description of the radiation pressure models used in this study and the main difference between them are given in Sect. 2. The reprocessing experiments realized to test the previous models and details on the power spectrum computation, widely used in this paper to analyze the errors at harmonics of the draconitic year, are described in Sect. 3. Finally, the GNSS geodetic products whose draconitic errors are analyzed in this study are the following: orbits (i.e. overlap errors, Sect. 4), geocenter Z-component (Sect. 5), Earth orientation parameters (Sect. 6) and station coordinates (Sect. 7).

2 Orbit models

2.1 CODE radiation pressure model

The CODE radiation pressure model is an empirical model to compensate the effect of SRP on GPS and GLONASS satellites. The model was first introduced by Beutler et al. (1994) where the extended orbit modeling techniques used by the Center for Orbit Determination in Europe (CODE) are

described. Up to nine empirical acceleration parameters can be estimated in a Sun-fixed orthogonal frame (Fig. 1):

$$D(u) = D_0 + D_C \cos u + D_S \sin u,$$
$$Y(u) = Y_0 + Y_C \cos u + Y_S \sin u,$$
$$B(u) = B_0 + B_C \cos u + B_S \sin u, \qquad (1)$$

where D points along the satellite-Sun direction, Y points along the solar panel beams (for nominal yaw attitude, explained in the next paragraph) and B completes the orthogonal frame. The main argument of the model is u, the argument of latitude of the satellite. This model is widely used within the IGS (International GNSS Service, Dow et al. 2009) community, in particular its 5-parameter version where only the D_0, Y_0, B_0, B_C and B_S parameters are estimated. In this study we also use this last version of the model.

The nominal yaw-steering attitude (the yaw angle Ψ is shown in Fig. 1) of the GPS and GLONASS satellites is given by accomplishing two conditions at the same time: (1) the antennas should be pointing to the center of the Earth to transmit the navigation signals and (2) the solar panels should be pointing perpendicular to the Sun to keep a maximum power supply.

2.2 Adjustable box-wing model

The adjustable box-wing model (Rodriguez-Solano et al. 2012b) was created to compensate the effects of SRP impacting GPS satellites, using an intermediate approach between the physical/analytical models and the purely empirical models. The box-wing model is based on the physical interaction between solar radiation and satellite surfaces, simplifying the satellite to a box (satellite bus) and to a wing (solar panels). In addition, nine parameters can be adjusted (estimated) to fit best the GPS tracking data just as the CODE model does. The nine parameters are:

1. solar panel scaling factor $(1 + \rho + \frac{2}{3}\delta)$,
2. solar panel rotation lag,
3. Y-bias acceleration (Y_0 of CODE model),
4. absorption plus diffusion ($\alpha + \delta$) of $+X$ bus,
5. absorption plus diffusion ($\alpha + \delta$) of $+Z$ bus,
6. absorption plus diffusion ($\alpha + \delta$) of $-Z$ bus,
7. reflection coefficient (ρ) of $+X$ bus,
8. reflection coefficient (ρ) of $+Z$ bus,
9. reflection coefficient (ρ) of $-Z$ bus.

The partial derivatives of the acceleration w.r.t. the previous parameters are written analytically (for the case of nominal yaw attitude of the GPS satellites) in Rodriguez-Solano et al. (2012b). The accelerations point towards the D and B directions for the first two parameters, if nominal yaw attitude is considered. The scaling factor of the solar panels just

Table 1 Solar radiation pressure and yaw attitude models selected for the 8 years (2004–2011) reprocessing experiments

[a] ftp://sideshow.jpl.nasa.gov/pub/GPS_yaw_attitude/nominal_yaw_rates

# Sol.	Solar radiation pressure	Yaw attitude
1	CODE 5-parameters	Nominal attitude law
2	Adjustable box-wing	Nominal attitude law
3	Adjustable box-wing	GPS-IIA: nominal yaw rates[a], Bar-Sever (1996)
		GPS-IIR: 0.20°/s yaw rate, Kouba (2009)
		GLONASS-M: 0.25°/s yaw rate, Dilssner et al. (2011)

differs from D_0 in the units and the solar panel rotation lag is a novel parameter which compensates for a small lag of the solar panels when they follow the Sun, about 1.5° and 0.5° respectively for the GPS-IIA and GPS-IIR satellites. Y_0 is identical to the same parameter of the CODE model. The last six parameters are the optical properties, divided into $\alpha + \delta$ and ρ, of the surfaces of satellite bus which are illuminated by the Sun under nominal yaw attitude conditions, namely the $+Z$, $+X$ and $-Z$ surfaces as shown in Fig. 1. For GLONASS satellites we tested adjustable box-wing models in Rodriguez-Solano et al. (2013), which are actually cylinder-wing models for the GLONASS (old type) and GLONASS-M satellites.

2.3 Yaw attitude models

During Sun–Earth eclipse seasons GPS and GLONASS satellites perform yaw maneuvers at orbit noon and orbit midnight, the first one happens in sunlight while the second one occurs in the shadow of the Earth. In particular, the GPS-II/IIA, GPS-IIR, GPS-IIF and GLONASS-M satellites perform these yaw maneuvers. Additionally, GPS-II/IIA satellites perform yaw maneuvers after shadow exit, usually called post-shadow maneuvers. Existing models describe precisely the yaw maneuvers performed by the GPS-II/IIA (Bar-Sever 1996), GPS-IIR (Kouba 2009), GPS-IIF (Dilssner 2010) and GLONASS-M (Dilssner et al. 2011) satellites. These models (except the one of GPS-IIF satellites) have been implemented in a development version of the Bernese GNSS Software (Dach et al. 2007, 2009).

If the navigation antenna of the satellite has an offset w.r.t. the satellite rotation axis (which is the case for GPS-II/IIA, GPS-IIF and GLONASS-M satellites) and the yaw maneuvers are not correctly modeled, large errors in the GNSS observations are introduced. Besides these geometrical effects, the SRP for the noon and post-shadow maneuvers will be mismodeled if the yaw maneuvers are not properly taken into account. During shadow maneuvers, Earth radiation pressure still acts on the satellites and should also be properly modeled. In Rodriguez-Solano et al. (2013) we upgraded the adjustable box-wing model to be able to work with non-nominal yaw attitude. However, the upgraded

model does not have any longer an analytical expression and has to be computed numerically for any arbitrary direction of the Sun w.r.t. the satellite surfaces.

3 Data analysis

3.1 Reprocessing experiments

For this study, we extended the first three orbit solutions computed in Rodriguez-Solano et al. (2013) from 2 years (2007–2008) to 8 years (2004–2011). This extension of the solutions allows us to better detect the draconitic errors in the computed geodetic products. We have computed three GPS+GLONASS solutions of eight years which differ only in the SRP and yaw attitude models as described in Table 1. We started from GPS and GLONASS cleaned observations and followed the strategy presented by Fritsche et al. (2014) with only minor differences described in detail in Rodriguez-Solano et al. (2013). The solutions are double-difference solutions. During the period 2004-2011 a maximum of 254 ground stations were reprocessed per day. Furthermore, the solutions computed for this study are individual 1-day solutions with no day boundary constraints applied. All the parameters of the CODE (5-parameter) and adjustable box-wing models (Sects. 2.1 and 2.2) are also estimated once per day. Together with the satellite orbits we have estimated the apparent geocenter coordinates, i.e., the offset between the instantaneous Earth's center of mass, as sensed by the satellites, and the reference frame origin (applying a no-net-translation condition). In Rodriguez-Solano et al. (2013) we computed five solutions where the last two included the real yaw attitude of GPS-IIA satellites obtained from PPP (Precise Point Positioning, Zumberge et al. 1997) phase residuals and a specific pitch attitude model for the solar panels of those satellites. The best orbit results were achieved with the last (fifth) solution, however, the largest improvements in the errors observed during eclipse seasons came with the Bar-Sever (1996) model with nominal yaw rates[1]. This is the reason why we only extended the first three solutions of Rodriguez-Solano et al. (2013) since the largest changes in the orbit

---

[1] ftp://sideshow.jpl.nasa.gov/pub/GPS_yaw_attitude/nominal_yaw_rates.

errors occurred within these three first solutions. Therefore, if exchanging the SRP and yaw attitude models has an impact on the draconitic errors observed in GNSS geodetic products, it should be observed within these three solutions.

The individual impact of GPS or GLONASS on the combined GPS+GLONASS solutions has not been evaluated in this study. This has been done in previous studies, e.g., Meindl et al. (2013) studied the impact on the geocenter while Fritsche et al. (2014) studied the impact on the station coordinates, satellite orbits and Earth orientation parameters. Nevertheless, the changes introduced by solution 3 are mainly due to changes in the orbit modeling of GPS-II/IIA satellites only. These satellites showed major improvements in the orbit overlap and prediction errors (Rodriguez-Solano et al. 2013) with the adjustable box-wing model upgraded for non-nominal yaw attitude, while GPS-IIR and GLONASS-M satellites only showed minor improvements. GLONASS (older block) satellites are unaffected as their yaw attitude during eclipse seasons is unknown and nominal yaw-steering attitude was used in all solutions. The changes observed in the geodetic parameters introduced by solution 2 are due to changes in the orbit modeling of both GPS and GLONASS satellites. The parameters of the CODE and adjustable box-wing models are significantly different (except D0 and Y0, see Sects. 2.1 and 2.2). Consequently the correlations within the model parameters and w.r.t. other parameters of the GPS+GLONASS solutions are also different. This study focuses mainly on the draconitic errors and on the changes due to the SRP and yaw attitude modeling. However, due to the different correlation of the models a redistribution of the errors into other estimated parameters or frequency bands cannot be ruled out.

3.2 Power spectrum

The power spectra, widely used in this paper to analyze the errors at harmonics of the draconitic year, are computed exactly as described in Rodriguez-Solano et al. (2012a). The power spectra are based on the Fast Fourier Transform (FFT, Press et al. 1992) and where data is missing, zero padding was employed, since GPS-derived daily estimates are evenly spaced. Moreover, the units of the power spectrum are well-defined (e.g. mm^2). Additionally, to compute the stacked (mean) power spectrum of the orbit overlap errors or of the stations coordinates a weighting according to the inverse of the variance was introduced to ensure that the noisier time series have a lower contribution. Our time series have a length of $T_S = 2,922$ days, i.e., 8 years. This means that one can reliably distinguish between estimated frequencies that are separated by $\Delta f = 0.125$ cpy. This is in accordance with Eq. (41) of Rothacher et al. (1999) which can be written as $\Delta f = 365.25/T_S$. Therefore, the 1st and 2nd draconitic harmonics at 1.04 and 2.08 cpy can be hardly dis-

tinguished from the annual and semiannual frequencies at 1 and 2 cpy. The separation of draconitic and annual harmonics starts to be reliable for the 3rd harmonic, where the separation of 0.12 cpy between harmonics almost reaches Δf. The separation between GPS and GLONASS draconitic harmonics starts to be reliable only for the 25th harmonic, i.e., as the respective frequencies are 26 and 25.875 cpy. Figures 2, 3, 4, 7 and 8 were created using the FFT approach with the number of tested frequencies equal to 4×2^{12}, where 12 is the next higher power of 2 of 2,922, such that the frequency interval in the figures is 0.0223 cpy. For the Tables 2, 4, 5 and 6 the numerical values of the power spectra at the draconitic harmonics were extracted from the respective figures by using a simple interpolation at the desired frequency values.

4 Impact on the orbit overlap errors

The orbit overlap errors, are an indicator of internal orbit consistency. Our daily satellite arcs span from 00:00:00 until 24:00:00, therefore our orbit overlaps are simply computed by taking the difference between consecutive 1-day arcs at the midnight epoch. The daily orbit overlaps were computed for the eight years we have (2004–2011) and for all GPS and GLONASS satellites. We then separated the orbit overlaps by Space Vehicle Number (SVN) and computed the individual power spectrum for each satellite as described in Sect. 3.2. The individual power spectra were stacked separately for GPS and GLONASS satellites using a weighting with the inverse of the variance of the orbit overlap errors to create Fig. 2.

For GPS satellite orbits we find large systematic errors at harmonics of one GPS draconitic year as already reported by Griffiths and Ray (2013). As we have expected from the results of Rodriguez-Solano et al. (2013) where we achieved significant reduction of the β_0 related orbit errors, the draconitic errors in the orbits also decrease with the new solar radiation pressure and attitude models. This can be seen in Fig. 2 but Table 2 is much more conclusive, where it can be seen that there is a general reduction of the errors. Moreover, if solutions 1 and 3 are compared directly in Table 2, we find a reduction of the errors for all the draconitic harmonics and for all the components. With an average[2] reduction of 46, 38 and 57 % for the the radial, along-track and cross-track components.

For GLONASS satellite orbits we find systematic errors at harmonics of one GLONASS draconitic year, at least for the first five harmonics as shown in Fig. 2. Here we find a mixture

---

[2] Over all the draconitic harmonics and weighted with the average values of solutions 1 and 3 such that small draconitic errors also have small contributions to the final average.
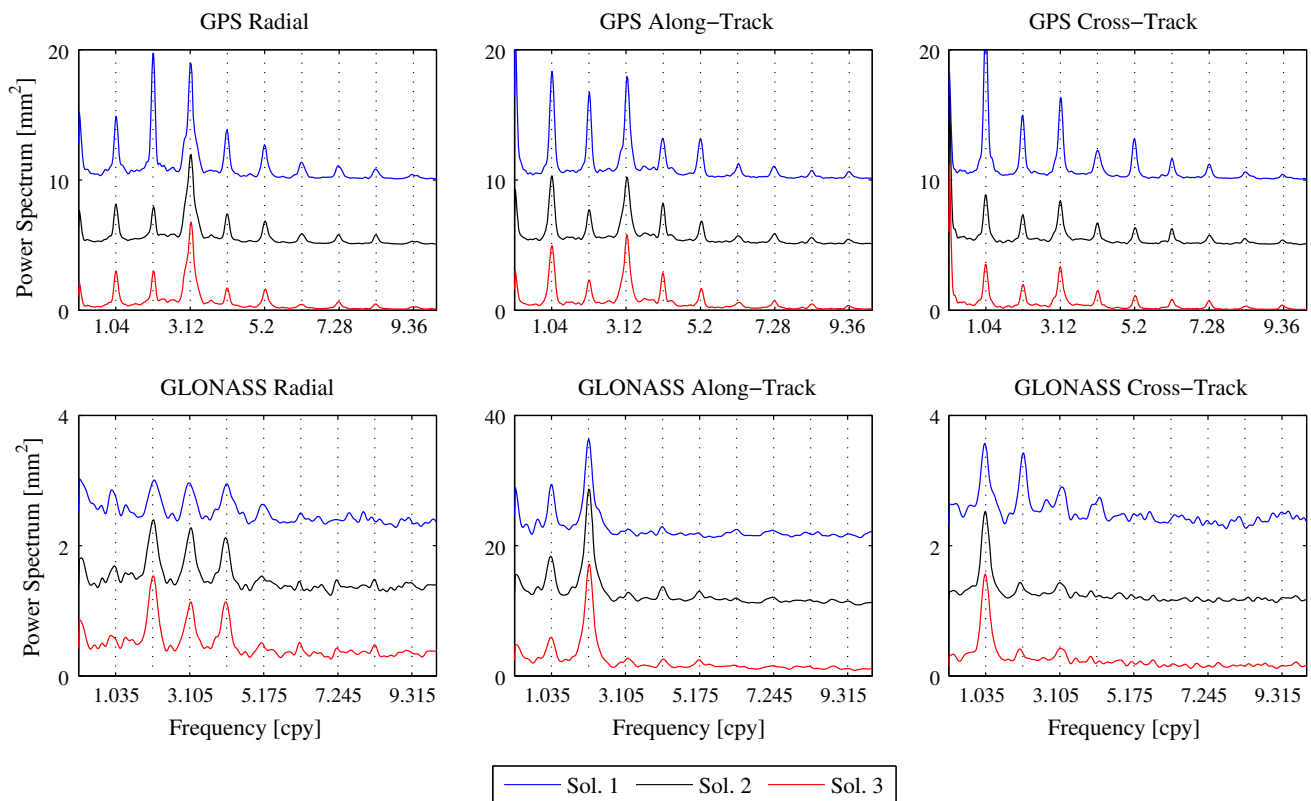
Fig. 2 Power spectrum of orbit overlap errors (stacked from all GPS and GLONASS satellites) for the three solutions given in Table 1 and separated in the radial, along-track and cross-track components. The power spectra of solutions 1 and 2 have been shifted along the *vertical axes* to make the details visible. The *dotted vertical lines* are at harmonics of 1.04 cpy for GPS and 1.035 cpy for GLONASS

Table 2 Numerical values (mm^2) of the GPS (left) and GLONASS (right) orbit overlap errors power spectra (see Fig. 2) at harmonics of 1.04 and 1.035 cpy

Comp.	# Sol.	1.04	2.08	3.12	4.16	5.20	6.24	7.28	8.32	9.36	1.035	2.07	3.105	4.14	5.175
Radial	1	4.71	9.66	8.90	3.71	2.69	1.34	1.05	0.82	0.37	0.76	0.98	0.96	0.95	0.63
Radial	2	*3.10*	*2.80*	*6.84*	*2.37*	*1.80*	*0.86*	*0.76*	*0.78*	*0.28*	*0.67*	**1.38**	**1.24**	**1.10**	*0.51*
Radial	3	*2.95*	**2.88**	*6.43*	*1.70*	*1.56*	*0.44*	*0.64*	*0.46*	*0.27*	*0.57*	**1.53**	*1.11*	**1.12**	*0.47*
Along	1	8.14	6.53	7.12	3.11	3.17	1.18	1.00	0.73	0.64	9.37	16.29	2.28	2.89	1.84
Along	2	*5.26*	*2.69*	*4.91*	**3.15**	*1.69*	*0.71*	*0.87*	*0.58*	*0.42*	*8.23*	**18.56**	**2.36**	**3.69**	**2.98**
Along	3	*4.90*	*2.31*	**5.46**	*2.79*	*1.55*	*0.56*	*0.72*	*0.48*	*0.34*	*5.88*	*16.90*	**2.43**	*2.55*	*2.43*
Cross	1	12.03	4.80	6.24	2.25	3.13	1.62	1.20	0.59	0.39	1.54	1.41	0.86	0.68	0.49
Cross	2	*3.84*	*2.28*	*3.41*	*1.69*	*1.31*	**1.26**	*0.74*	*0.43*	*0.36*	*1.51*	*0.38*	*0.43*	*0.22*	*0.22*
Cross	3	*3.51*	*1.95*	*3.34*	*1.48*	*1.09*	*0.83*	*0.70*	*0.32*	*0.34*	**1.55**	*0.35*	*0.42*	*0.20*	*0.20*

Italic indicates an improvement w.r.t. the previous solution while bold indicates a degradation

of improvement and degradation in the errors when using the new solar radiation pressure and attitude models, see Table 2. We obtain an average[2] reduction of the errors of 5 and 39 % for the along-track and cross-track components, while in the radial component the errors are increased in average by 16 %. Mainly the cross-track component shows a general improvement, in all but the 1st harmonic which is slightly degraded.

In Rodriguez-Solano et al. (2013) the cross-track component was also the one with the highest improvements. The fact that the draconitic errors in the radial and along-track components are almost not improved or even degraded (contrary to GPS) suggests that the adjustable box-wing models for GLONASS satellites could be further improved. For example, the parameter constraints which were initially selected
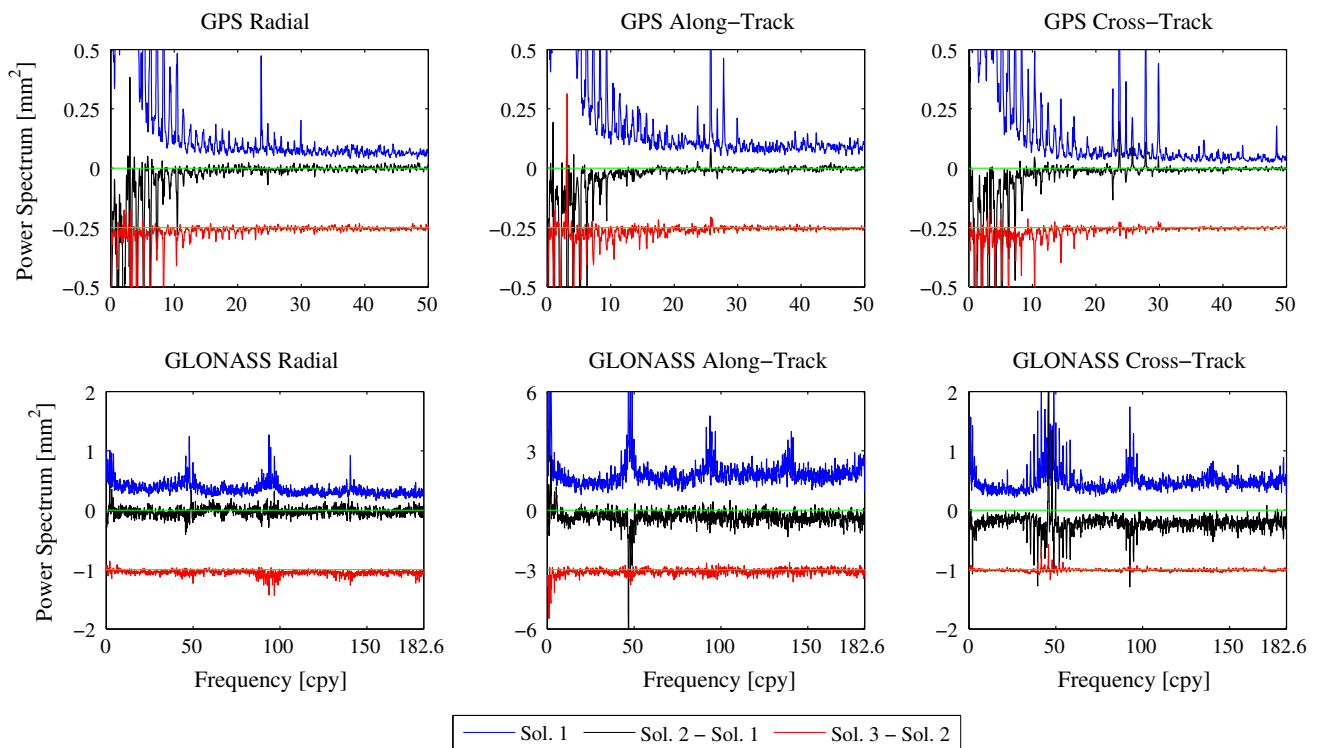
Fig. 3 Same as Fig. 2 for solution 1 but extended until 50 cpy for GPS and until 182.625 cpy (Nyquist frequency) for GLONASS. Additionally, the differences of the power spectra of consecutive solutions are shown, the last ones have been shifted along the *vertical axes*. Negative values (below the *green lines*) indicate an improvement w.r.t. the previous solution while positive values indicate a degradation

for GPS satellites (Rodriguez-Solano et al. 2012b) may be less appropriate for GLONASS satellites.

The power spectra of the orbit overlap errors were also stacked separately (not shown) for GPS-II/IIA, GPS-IIR, GLONASS (older block) and GLONASS-M satellites. There are no large differences between the power spectra of GPS-II/IIA or GPS-IIR satellites (except for few peaks) and the power spectra shown in Fig. 2 correspond essentially to simple averages of the two power spectra. For GLONASS satellites the situation is very different, the power spectra (and the orbit overlap errors) of all components are larger for GLONASS (older block) than for GLONASS-M satellites. Due to the weighting with the inverse of the variance used for stacking the power spectra of the satellites, the GLONASS (older type) satellites have a small contribution to the power spectra shown in Fig. 2. Furthermore, the draconitic errors in the along-track component of the GLONASS (older type) satellites are in general increased (especially for the 2nd harmonic) with the adjustable box-wing model.

While the main focus of this paper is on the low draconitic harmonics, we consider important to include here also the power spectra of orbit overlap errors at higher frequencies (Fig. 3). In particular for GLONASS, there are some striking patterns in the power spectra of the orbits, like the clusters of peaks around 47, 94 and 140 cpy. At the moment we do not

have an explanation for these features but the first frequency is close to eight sidereal days or 45.8 cpy, the repeat period of the GLONASS ground tracks. Besides these features it is interesting to note in Fig. 3 that the power spectra are generally decreased when using the adjustable box-wing model, in particular for the cross-track component. From Table 2 one cannot affirm that the adjustable box-wing model brings a general improvement in the radial and along-track components of the GLONASS orbits, but this can be affirmed looking at Fig. 3 and at Table 3. For GPS orbits most of the power concentrates at the low frequencies, besides the draconitic harmonics we find high peaks between 20 and 50 cpy, most probably related to errors of the sub-daily EOP tide model as discussed by Griffiths and Ray (2013). As shown in Fig. 3, some of these peaks are amplified and some reduced especially for the cross-track component and between 20 and 30 cpy when the adjustable box-wing model is used. Beyond 50 cpy (not shown for GPS) there is only white noise, with just a small degradation in the radial component at very high frequencies when the adjustable box-wing model is used. Nevertheless, the new models reveal a general improvement in the GPS orbit overlap errors as shown in Table 3. For the other GNSS geodetic products analyzed in this paper, i.e., geocenter Z-component, Earth orientation parameters and stations coordinates, we did not find significant differences

Table 3 RMS of the orbit overlap errors (mm) over all GPS and GLONASS satellites, weighted with the inverse of the variance of each satellite

Component	# Sol.	GPS	GLONASS
Radial	1	32.20	66.93
Radial	2	*31.07*	**67.71**
Radial	3	*30.05*	*62.13*
Along	1	37.17	163.78
Along	2	*34.04*	*147.59*
Along	3	*33.34*	*140.50*
Cross	1	30.04	83.32
Cross	2	*26.74*	*62.68*
Cross	3	*25.67*	*61.57*

Italic indicates an improvement w.r.t. the previous solution while bold indicates a degradation

in the power spectra of the solutions given in Table 1 at high frequencies. Therefore, we did not include such figures in this paper.

5 Impact on the geocenter Z-component

The geocenter Z-component estimated with the CODE (5-parameter) radiation pressure model shows large variations that can be (visually) correlated with the β_0 angle of the different orbital planes as shown in Fig. 4. This correlation is particularly strong with the GLONASS β_0 angles in the last years of the time series. The power spectrum of the geocenter Z-component shows strong draconitic errors at odd harmonics of 1.04 cpy. In comparison, the draconitic errors of the geocenter X and Y components (Fig. 5) are much less significant. We cannot make a distinction between the specific GPS and GLONASS draconitic errors as the fundamental frequencies of the harmonics (1.04 and 1.035 cpy) are very close to each other, see also Sect. 3.2. Exchanging the CODE (5-parameter) radiation pressure model by the adjustable box-wing model results in a significant reduction of the geocenter Z-component variations and of the associated draconitic errors (solutions 1 and 2 in Fig. 4 and Table 4). The possibility that the CODE model can cause these problems in the geocenter was already discussed by Meindl et al. (2013) as follows:

"Having said that orbit parametrization plays an important role one might conclude that the problems encountered in this article are uniquely caused by the CODE orbit model (5), (6). This is not true, however: Alternative models, like, e.g., box-wing models, cannot live without model parameters, which have to be determined in the parameter estimation process. Our theory asks that each empirical acceleration standing behind such a free parameter has to be decomposed into the

(R, S, W)[3]-components-along the lines presented in Sect. 2.2. As soon as W-components with non-zero means over a revolution result, there is the danger of generating artifacts."

We agree with the previous paragraph and indeed our adjustable box-wing model does have model parameters that have to be estimated in the orbit determination process as mentioned in Sect. 2.2 of this paper. However, those parameters with exception of D_0 and Y_0 are significantly different from the CODE model parameters. The D_0 acceleration has a non-zero mean in the W-component while Y_0 does not have one. In what follows we will analyze the box-wing model parameters which could have a W-component.

The solar panel rotation lag acceleration points in the B-direction (see Fig. 1) and has a main dependency on sign($\dot{\epsilon}$), given in Eq. (15) of Rodriguez-Solano et al. (2012b), which can be approximated as $\sin(\mu)$. Where μ (see Fig. 1) is the orbit angle formed between the spacecraft position vector and orbit midnight, growing with the satellite's motion (Bar-Sever 1996). According to Eq. (16) of Meindl et al. (2013), the W-component of a constant B acceleration can be written as:

$$W_{\rm B} = B \frac{- \sin 2\beta_0 \cos \mu}{2\sqrt{1 - \cos^2 \beta_0 \cos^2 \mu}}. \tag{2}$$

Multiplying the last equation with sign($\dot{\epsilon}$) or $\sin(\mu)$ results in a twice-per-revolution term with zero mean acceleration. Meindl et al. (2013) noted that the once-per-revolution empirical parameters in the Y-direction of the CODE model [Eq. (1)] result in a superposition of a constant and a twice-per-revolution term in the W-component which can be very problematic for the geocenter estimation. However, in that paper it was not noted that it is the same case for the once-per-revolution empirical parameters in the B-direction of the CODE model [Eq. (1)], which can perfectly generate a $\cos(\mu)$ term that multiplied with Eq. (2) also results in a superposition of a constant and a twice-per-revolution term. This coincides with the results of Rebischung et al. (2014) who found that the simultaneous estimation of the D_0, B_C and B_S from the CODE (5-parameter) radiation pressure model slightly increases the estimation problems of the geocenter Z-component.

The absorption plus diffusion parameters of the adjustable box-wing model show large correlations to other box-wing parameters if they are freely estimated. Therefore, as described in Rodriguez-Solano et al. (2012b) those parameters are tightly constrained in the orbit determination process and consequently should have a minimal impact on the geocenter estimation. However, the reflection parameters are estimated with loose constrains. The $+Z$ and $-Z$ directions

---

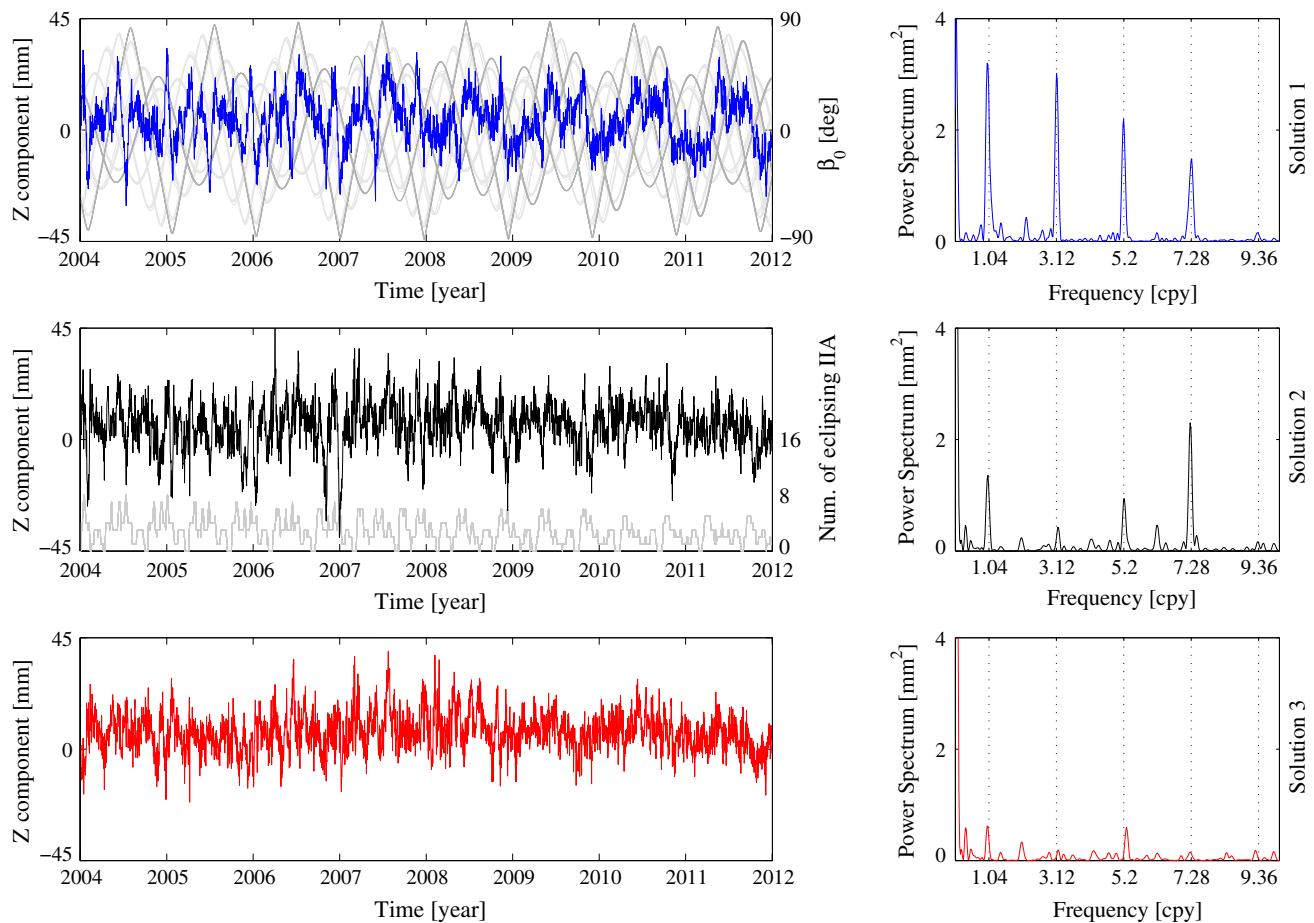[3] The RSW components are defined as: radial (R), along-track (S) and cross-track (W).

Fig. 4 Time series of the daily estimated Z-component geocenter for the three solutions given in Table 1. On the right, the power spectrum of the corresponding time series is shown. The *dotted vertical lines* are at harmonics of 1.04 cpy. In the background of the time series of solution 1, the Sun elevation angle above the orbital plane (β_0) of all GPS (*light gray*) and GLONASS (*dark gray*) satellites is displayed. In the background of the time series of solution 2, the number of GPS block II and IIA in eclipse season is displayed. During the time period from 2004 until 2011, a maximum number of 8 GPS block II and IIA satellites were simultaneously in eclipse season

are parallel to the radial direction, such that the only parameter which could have a cross-track component is the one pointing along the $+X$ direction, see Fig. 1. This parameter has a main dependency on $\sin^2(\epsilon)$, given in Eq. (12) of Rodriguez-Solano et al. (2012b), which can be written as:

$$\sin^2 \epsilon = 1 - \cos^2 \beta_0 \cos^2 \mu. \tag{3}$$

The W-component of a constant X acceleration can be written as:

$$W_X = X \frac{\sin \beta}{\sqrt{1 - \cos^2 \beta_0 \cos^2 \mu}}. \tag{4}$$

Multiplying the last equation with $\sin^2(\epsilon)$ results in a twice-per-revolution term with non-zero mean acceleration.

Summarizing, the CODE (5-parameter) radiation pressure model has the D_0, B_C and B_S parameters which could cause problems for the geocenter estimation, while for the adjustable box-wing model the problematic parameters are

the solar panel scaling factor and the reflection coefficient of the $+X$ bus surface. Therefore, according to the theory developed by Meindl et al. (2013) the differences in the geocenter estimates between solutions 1 and 2 in Fig. 4 should mainly result from replacing the once-per-revolution B parameters by the $+X$ reflection parameter. Both type of parameters generate twice-per-revolution with non-zero mean cross-track accelerations. However, with the fundamental difference that the acceleration generated from the once-per-revolution parameters in B-direction is purely empirical while the acceleration due to $+X$ reflection results from the physical interaction between the Sun and the $+X$ surface. Moreover, with the adjustable box-wing model we obtained improvements in the cross-track components of the GPS orbits and especially of the GLONASS orbits as shown in Sect. 4. This parametrization difference is, from our point of view, the explanation of the improvement obtained in the geocenter Z-component estimation with the adjustable box-wing model.
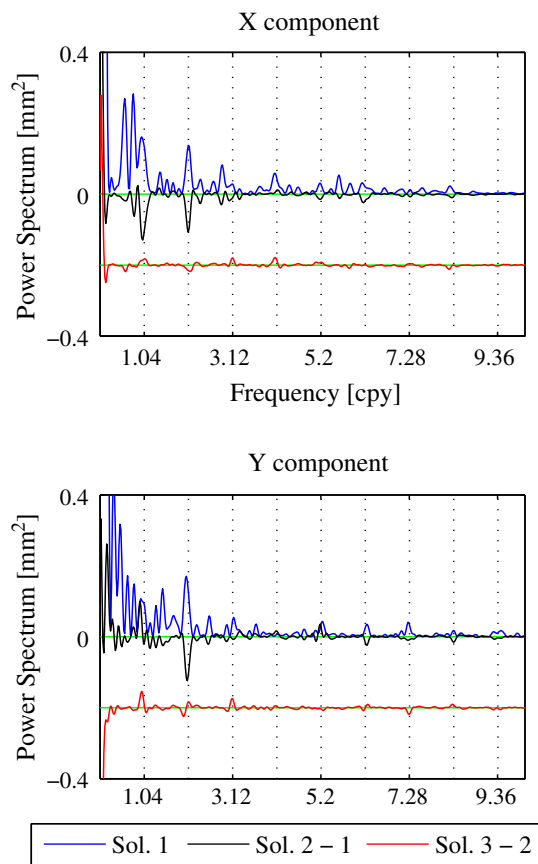
X component

Y component

Fig. 5 Power spectrum of the geocenter X and Y components for solution 1. Additionally, the differences of the power spectra of consecutive solutions are shown, the last ones have been shifted along the *vertical axes*. Negative values (below the *green lines*) indicate an improvement w.r.t. the previous solution while positive values indicate a degradation. The *dotted vertical lines* are at harmonics of 1.04 cpy

Table 4 Numerical values (mm^2) of the geocenter power spectrum (see Fig. 4) at odd harmonics of 1.04 cpy

Component	# Sol.	1.04	3.12	5.20	7.28	9.36
Z	1	2.30	2.97	2.14	1.45	0.13
Z	2	*1.00*	*0.25*	*0.94*	**2.00**	**0.14**
Z	3	*0.37*	*0.08*	*0.13*	*0.13*	*0.02*

Italic indicates an improvement w.r.t. the previous solution while bold indicates a degradation

We do not have an explanation about why the CODE radiation pressure model generates draconitic errors in the geocenter just at odd harmonics. However, we believe to have an explanation on the largest (7th) harmonic observed on solution 2, computed with the adjustable box-wing model with nominal yaw attitude. Solution 2 has mainly large orbit errors during eclipse seasons, which as mentioned in the Introduction happen twice per draconitic year. The GPS system, the one contributing the most to the geocenter computation as shown by Meindl et al. (2013), has six orbital planes equally
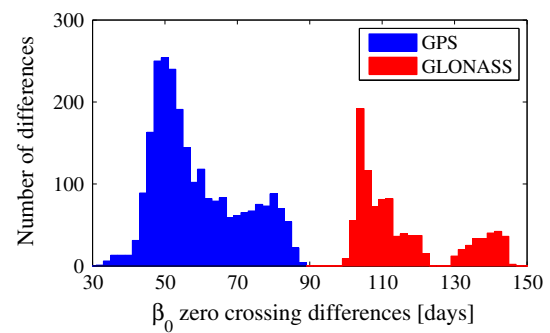

Fig. 6 Histogram of differences in days between β_0 zero crossing points ($\beta_0 = 0°$, see also Fig. 4) of consecutive orbital planes during the time period 2004–2011, separately for GPS and GLONASS

spaced along the equator. Thus one would intuitively expect the largest draconitic harmonic to be at the 6th harmonic, obviously this is not the case when looking at Fig. 4. Why the largest peak is at the 7th and not at the 6th harmonic may be explained through Fig. 6 which shows the histograms of differences in days between consecutive GPS orbital planes along the ecliptic (not the equator). The peak of this histogram is at about 50 days which would correspond to the 7th draconitic harmonic. Sun–Earth eclipses last at maximum 1 h for a GPS satellite orbital revolution, and a satellite is in eclipse season around 73 days (average over 6 orbital planes) during 1 year. While these time periods seem small, the complete arc for an eclipsing satellite may be degraded. Moreover, the GPS consists of six different orbital planes, which increases the probability that for any day at least one GPS-II/IIA satellite is in eclipse season. This is shown in the background of the time series of solution 2 in Fig. 4. Moreover, one or few of the satellites with worse orbits than others can have a negative impact on a global GNSS solution and consequently on the geocenter estimation. As we would have expected, solution 3, which reduces the orbit errors during eclipse seasons mainly for GPS-IIA satellites, reduces very significantly the 7th draconitic harmonic when compared to the previous solution as shown in Fig. 4.

Finally, as in the case of the GPS orbits (Table 2), for the geocenter Z-component there is an overall reduction of the draconitic errors when the new SRP and yaw attitude models are used. The less significant draconitic errors in the X and Y components (Fig. 5) show mainly a reduction in the 1st and 2nd harmonics of the X-component and in the 2nd harmonic of the Y-component when using the adjustable box-wing model. When comparing solutions 1 and 3 (Fig. 4; Table 4) it can be observed that the errors almost disappear for all the draconitic harmonics of the geocenter Z-component, with an average^2 reduction of 92 %.

The geocenter Z-component from geodetic estimates and geophysical models show a predominant annual signal with an amplitude of 3–5 mm (see e.g. Wu et al. 2012). This annual
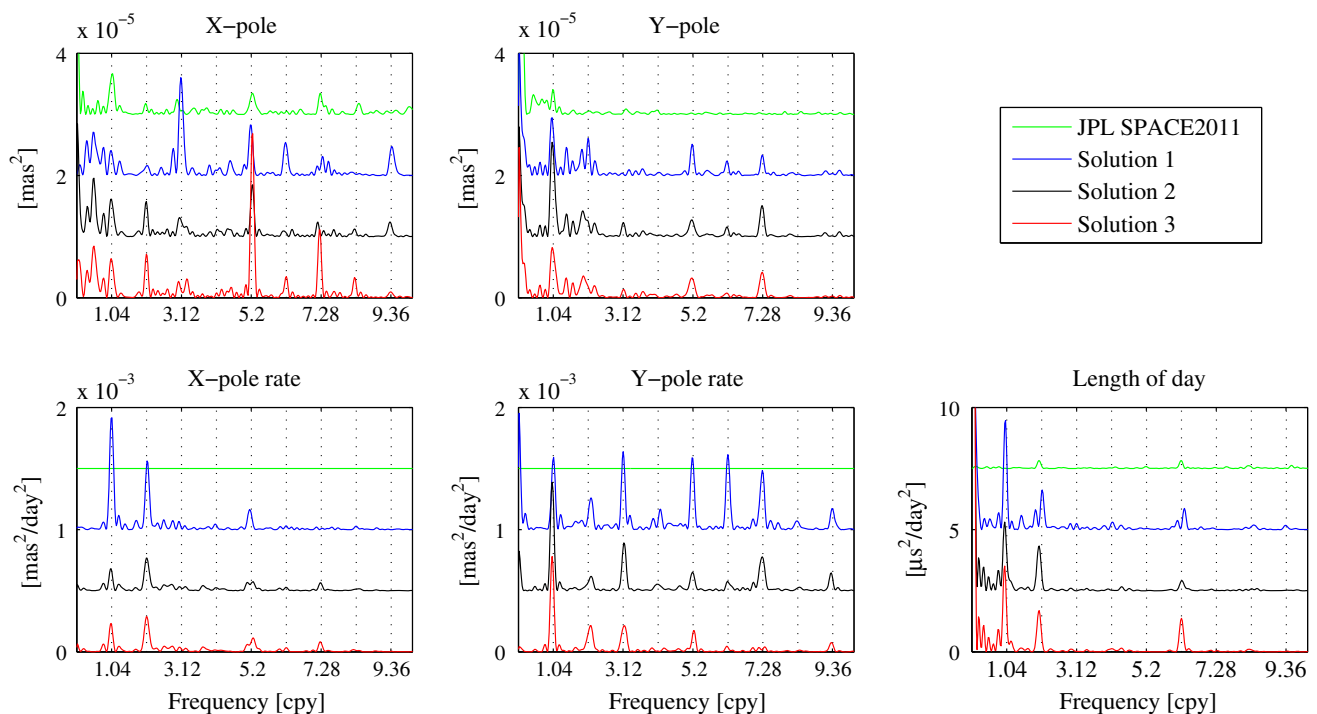
Fig. 7 Power spectrum of the Earth orientation parameters (minus IERS 08 C04 time series) for JPL SPACE2011 and the three solutions given in Table 1. The power spectra of JPL SPACE2011 and solutions 1 and 2 have been shifted along the *vertical axes* to make the details visible. The differences between JPL SPACE2011 and IERS 08 C04 are at the level of 10^{-7} mas^2/day^2 for the pole rates. The *dotted vertical lines* are at harmonics of 1.04 cpy. The power spectrum of UT1-UTC is not shown since in our GNSS solutions these values are fixed to IERS 08 C04 at the beginning of each day

signal is not visible for solution 3 in Fig. 4. The time series of the geocenter Z-component from our best solution (3) still have a noise much larger than 5 mm. The respective power spectrum shows a peak close to the annual period but significant power can still be found at other frequencies. We fitted a harmonic signal with annual period to the time series, but the standard deviation of the time series minus the fit just showed a minimal decrement compared to the standard deviation of the time series. These findings suggest that despite the large reduction of the draconitic errors obtained for the geocenter Z-component, corresponding estimates are still subject to remaining modeling errors. Inherent problems of the GNSS technique to estimate the geocenter coordinates, like the high collinearity with the estimated satellite clock and troposphere parameters (Rebischung et al. 2014), could be limiting factors to further reduce the errors found in the GNSS-derived geocenter Z-component.

6 Impact on the Earth orientation parameters

Seitz et al. (2012) found draconitic harmonics in the Y-pole rate of GPS minus VLBI (Very Long Baseline Interferometry) time series. High peaks in the power spectrum were present at 50 and 70 days corresponding to the 7th and 5th harmonics of the GPS draconitic year. In the power spectrum of the X-pole rate the 5th and 7th peaks were also present but with a much lower magnitude. In this study we compared the GNSS-derived EOP (Earth Orientation Parameters) with external sources like the IERS 08 C04[4] (International Earth Rotation and Reference Systems Service, Bizouard and Gambis 2009) and the JPL SPACE2011[5] (Jet Propulsion Laboratory, Ratcliff and Gross 2013) time series, as the draconitic harmonics of the solutions alone were not clearly visible. When subtracting IERS 08 C04 or JPL SPACE2011 the draconitic harmonics become visible. However, the interpretation of the results is difficult as the IERS 08 C04 and JPL SPACE2011 time series contain GPS data which may also include draconitic errors. Moreover, the IGS Analysis Centers[6] contributing to the EOP combinations use different SRP models.

Figure 7 shows the power spectra of the three solutions computed in this study (Table 1) minus the IERS 08 C04

[4] ftp://hpiers.obspm.fr/iers/eop/eopc04.

[5] ftp://euler.jpl.nasa.gov/keof/combinations/2011.

[6] The analysis strategy summaries can be found at: ftp://igscb.jpl.nasa.gov/pub/center/analysis/.

Table 5 Numerical values of the Earth orientation parameters power spectra (w.r.t. IERS 08 C04, see Fig. 7) at significant harmonics of 1.04 cpy

Component	# Sol.	1.04	2.08	3.12	4.16	5.20	6.24	7.28	8.32	9.36
X-pole	1		0.16	1.55		0.81	0.51	0.20		0.44
X-pole	2		**0.56**	*0.25*		*0.70*	*0.06*	*0.01*		*0.22*
X-pole	3		**0.71**	*0.11*		**2.25**	**0.34**	**0.80**		*0.09*
X-pole rate	1	0.91	0.52			0.13		0.01		
X-pole rate	2	*0.16*	*0.27*			*0.06*		**0.06**		
X-pole rate	3	**0.22**	**0.29**			**0.08**		**0.08**		
Y-pole	1	0.72	0.60			0.48		0.32		
Y-pole	2	**1.37**	*0.24*			*0.25*		**0.49**		
Y-pole	3	*0.76*	*0.18*			**0.30**		*0.41*		
Y-pole rate	1	0.58	0.13	0.63	0.07	0.57	0.61	0.47	0.07	0.17
Y-pole rate	2	**0.74**	*0.07*	*0.35*	*0.05*	*0.15*	*0.08*	*0.27*	*0.02*	*0.11*
Y-pole rate	3	*0.63*	**0.15**	*0.20*	*0.01*	0.15	*0.04*	*0.02*	*0.01*	*0.07*
Length of day	1	3.04	1.52				0.11			
Length of day	2	*1.55*	*0.77*				**0.40**			
Length of day	3	**1.64**	*0.73*				**1.35**			

The units are 10^{-5} mas^2 for pole values, 10^{-3} mas^2/day^2 for pole rates and μs^2/day^2 for LOD. Italic indicates a decrement w.r.t. the previous solution while bold indicates an increment

time series. Additionally, the power spectrum of the JPL SPACE2011 minus IERS 08 C04 time series is displayed for comparison purposes. The power spectrum of the difference of these two external EOP time series sets a lower limit for the comparison of our solutions w.r.t. IERS 08 C04. Draconitic harmonics amplitudes above this limit can be interpreted as significant (i.e. as an error in our solutions) while below or close to this limit the amplitudes can be interpreted as insignificant as they also exist between other EOP time series. Figure 7 shows that the draconitic errors in the X and Y pole as well as in the LOD (length of day) are generally close to this lower limit with some harmonics exceeding it. Table 5 shows a similar number of cases with improvements and degradations in the draconitic harmonics when comparing solutions 1 and 3 for the X and Y pole as well as for the LOD. We obtain an average^2 increase of the errors of 115 and 149 % for the X-pole and LOD, while the errors in the Y-pole are reduced in average by 15 %. The main contributor to the increase of the draconitic errors in the X-pole is the 5th harmonic while for the LOD it is the 6th harmonic. We do not have, at the moment, an explanation for the increase of the amplitudes of these particular harmonics. For the X and Y pole rates the draconitic harmonics are very significant, as shown in Fig. 7. Here the differences between JPL SPACE2011 and IERS 08 C04 are at the level of 10^{-7} mas^2/day^2, i.e., four orders of magnitude smaller than the differences between our solutions and IERS 08 C04. Table 5 shows that there are more cases with improvements than degradations in the draconitic harmonics of the X and Y pole rates. With an average^2 reduction of the

errors between solutions 1 and 3 of 24 and 50 % for the X and Y pole rates.

We also computed the power spectra of the pole and pole-rates separately for prograde and retrograde motions (not shown) obtaining the highest differences to IERS 08 C04 at draconitic harmonics for the prograde motion rate. However, we decided to show here the pole and pole-rates for the X and Y components since the draconitic harmonics in the X-pole and Y-pole rate are much more dominant than in the Y-pole and X-pole rate, see Fig. 7 and Table 5. This asymmetry suggests a possible relation with the distribution of GNSS ground stations over the Earth, as the X and Y components are given in an Earth-fixed system.

7 Impact on the station coordinates

The power spectra of GPS-derived station coordinates show spurious signals at harmonics of one GPS draconitic year as first noted by Ray et al. (2008). At least until the 9th harmonic these spurious signals are visible as shown in the power spectra of our GNSS-derived station coordinates in Fig. 8. Rodriguez-Solano et al. (2012a) obtained a reduction of 38 % only in the 6th harmonic of the North component when introducing the Earth radiation pressure in the computation of GPS satellite orbits. In this study, the 6th harmonic of the North component is reduced (after subtracting a noise floor of 0.00069 mm^2, see Table 6) by 32 % when using the adjustable box-wing model for GPS and GLONASS satel-
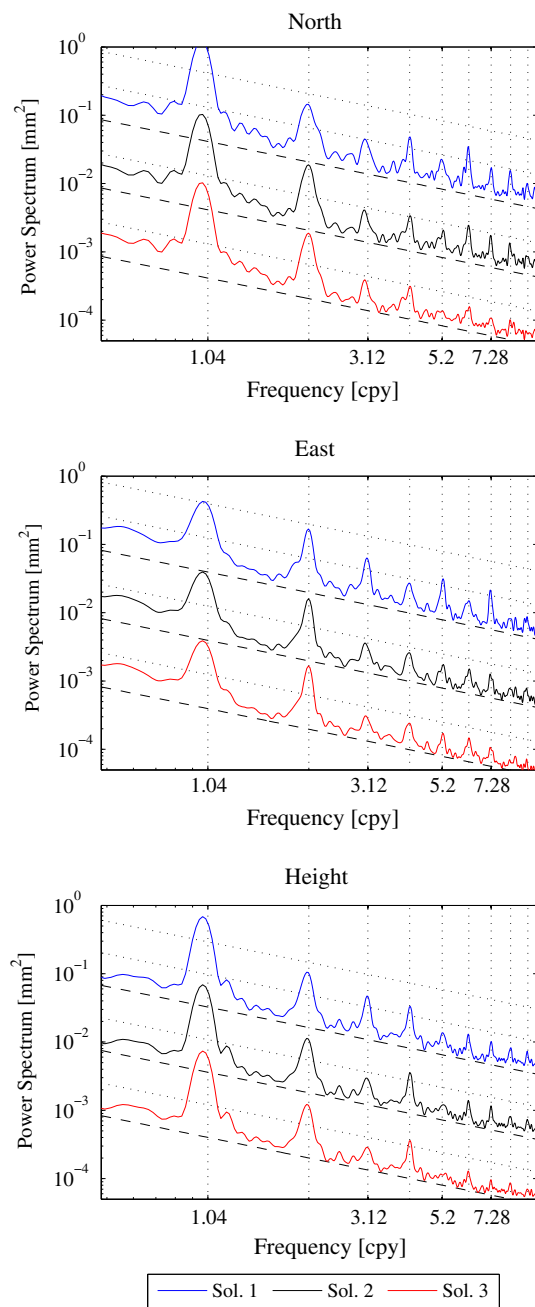
Fig. 8 Power spectrum of daily station coordinates (stacked from around 290 ground stations) for the three solutions given in Table 1 separately for the North, East and Height components. The power spectra of the solutions have been shifted along the *vertical axes* to make the details visible. The *dotted vertical lines* are at harmonics of 1.04 cpy. The sloped lines have a power law behavior of $1/f$ (i.e. flicker noise), the *dashed lines* represent approximate noise floors

lites. Another 53 % (see footnote[7]) reduction (w.r.t. solution 2) is achieved with the upgraded version of the model based on non-nominal yaw attitude. In total, comparing solutions

1 and 3, a reduction of 68 % (see footnote 7) is achieved for the 6th harmonic in the North component. However, in this study with the new radiation pressure and yaw attitude models not only this peak is reduced but we achieve a general reduction of the draconitic errors in the station coordinates as shown in Fig. 8. In fact, when comparing solutions 1 and 3 in Table 6, it can be observed that all the draconitic harmonics (except the 2nd harmonic in the North component) are reduced in the North, East and Height components. We obtain an average reduction over all the draconitic errors between solutions 1 and 3 of 41, 39 and 35 % (see footnote 7) for the North, East and Height components after subtracting the approximate noise floors given in Table 6. Moreover, the weighted RMS over all station coordinates (Table 7) also shows a decrement in the North, East and Height components with the new models.

The impact of the new radiation pressure and yaw attitude models on the station coordinates can also be analyzed by looking at the time series of station coordinates. We did not look at the time series of individual ground tracking stations, but we computed the RMS of the differences of daily station coordinates (between one solution and the previous one) as a function of time as shown in Fig. 9. It can be noted that the adjustable box-wing model has a higher impact on the station coordinates (especially in the North and East components) than its upgraded version for non-nominal yaw attitude. However, this last model causes a very systematic behavior, namely a nearly vanishing RMS difference when there are no GPS-II/IIA in eclipse seasons, see also Fig. 4. The RMS difference is not exactly zero since solution 3 includes the yaw bias for GPS-II/IIA satellites (Bar-Sever 1996) which also acts outside of eclipse seasons, as well as specific yaw attitude models for eclipsing GPS-IIR and GLONASS-M satellites (Table 1). When GPS-II/IIA satellites are in eclipse season large differences appear in the station coordinates. Obviously one or few of the satellites with degraded orbits can have a negative impact on a global GNSS solution and consequently on the station coordinates.

8 Conclusions

Part of the draconitic errors found in GNSS geodetic products are definitely induced by orbit modeling deficiencies, in particular those related to the radiation pressure modeling. We have shown that by changing the radiation pressure models also the draconitic errors show important changes. By exchanging the CODE (5-parameter) radiation pressure model (Beutler et al. 1994) by our adjustable box-wing model (Rodriguez-Solano et al. 2012b) orbit related systematic errors with a β_0 (Sun elevation angle above the orbital plane) dependency are reduced outside eclipse seasons for GPS-IIA, GPS-IIR and GLONASS-M satellites as shown by

---

[7] This reduction may not be easily seen in Fig. 8 due to the logarithmic scale, but it can be computed from the numerical values given in Table 6.

Table 6 Numerical values (mm^2) of the station coordinates power spectra (see Fig. 8) at the harmonics of 1.04 cpy

Component	# Sol.	1.04	2.08	3.12	4.16	5.20	6.24	7.28	8.32	9.36
North	1	0.08639	0.01413	0.00378	0.00479	0.00221	0.00328	0.00170	0.00152	0.00095
North	2	*0.07365*	**0.01865**	*0.00296*	*0.00333*	*0.00187*	*0.00244*	*0.00166*	*0.00116*	*0.00085*
North	3	*0.07330*	*0.01858*	*0.00294*	*0.00309*	*0.00136*	*0.00152*	*0.00107*	*0.00097*	*0.00063*
North	η/f	0.00413	0.00207	0.00138	0.00103	0.00083	0.00069	0.00059	0.00052	0.00046
East	1	0.03796	0.01655	0.00611	0.00269	0.00291	0.00150	0.00190	0.00082	0.00078
East	2	*0.03300*	*0.01569*	*0.00310*	*0.00257*	*0.00163*	*0.00146*	*0.00112*	*0.00075*	*0.00063*
East	3	*0.03248*	**0.01636**	*0.00281*	*0.00240*	**0.00165**	0.00146	*0.00100*	*0.00065*	*0.00055*
East	η/f	0.00394	0.00197	0.00131	0.00099	0.00079	0.00066	0.00056	0.00049	0.00044
Height	1	0.54979	0.10067	0.04660	0.03263	0.01362	0.01259	0.01012	0.00823	0.00674
Height	2	*0.49564*	*0.09628*	*0.02588*	*0.03140*	*0.01073*	*0.01222*	**0.01033**	*0.00727*	*0.00639*
Height	3	*0.48429*	*0.09339*	*0.02298*	*0.02883*	*0.00920*	*0.01017*	*0.00765*	*0.00692*	*0.00561*
Height	η/f	0.03250	0.01625	0.01083	0.00812	0.00650	0.00542	0.00464	0.00406	0.00361

Italic indicates an improvement w.r.t. the previous solution while bold indicates a degradation. Additionally, the value of the power law η/f (i.e. flicker noise) with $\eta = [0.0043, 0.0041, 0.0338]$ is included, representing approximate noise floors (dashed lines in Fig. 8) for the respective components

Table 7 RMS over all daily station coordinates (mm), weighted with the inverse of the variance of each station

Component	# Sol.	WRMS
North	1	2.10
North	2	*2.05*
North	3	*2.02*
East	1	1.88
East	2	*1.84*
East	3	*1.82*
Height	1	5.69
Height	2	*5.60*
Height	3	*5.55*

Italic indicates an improvement w.r.t. the previous solution

Rodriguez-Solano et al. (2013). However, the orbit errors during eclipse seasons are increased especially for GPS-IIA satellites if the yaw maneuvers of these satellites are not properly taken into account. In Rodriguez-Solano et al. (2013) we upgraded the adjustable box-wing model to use non-nominal yaw attitude, i.e., to use the Bar-Sever (1996), Kouba (2009) and Dilssner et al. (2011) yaw attitude models. With this an important improvement of the orbits (in particular for GPS-IIA satellites) was achieved during eclipse seasons. These improvements in the orbits, especially because related to

the β_0 angle, were expected to reduce the draconitic errors observed in diverse GNSS geodetic products. In this study, we show that this is in fact the case. With the new radiation pressure models (Rodriguez-Solano et al. 2012b, 2013) we obtained a reduction of the draconitic errors in the orbits (overlap errors), in the geocenter Z-component, in the X and Y pole rates, and in the station coordinates. The draconitic errors for the X and Y pole as well as for the LOD are not that significant as for the pole rates and the results are not conclusive when using the new models. In Rodriguez-Solano et al. (2013) we showed that there are still β_0 systematic errors present in the GPS and GLONASS orbits, even after using the new models. Therefore, a large potential to further reduce the draconitic errors in the GNSS geodetic products exists if the β_0 systematics in the orbits can be further reduced. The draconitic errors observed in the geocenter Z-component tend to disappear with the new radiation pressure models and it can be concluded that the observed odd harmonics were introduced by the CODE 5-parameter model. However, we cannot conclude that only radiation pressure orbit modeling deficiencies contribute to the draconitic errors observed in the station coordinates, in the Earth rotation parameters or in the orbits themselves. Other error sources like multipath or mismodeling of sub-daily signals could be contributing to the observed draconitic errors. These other error sources cannot be ruled out by the results of this study.
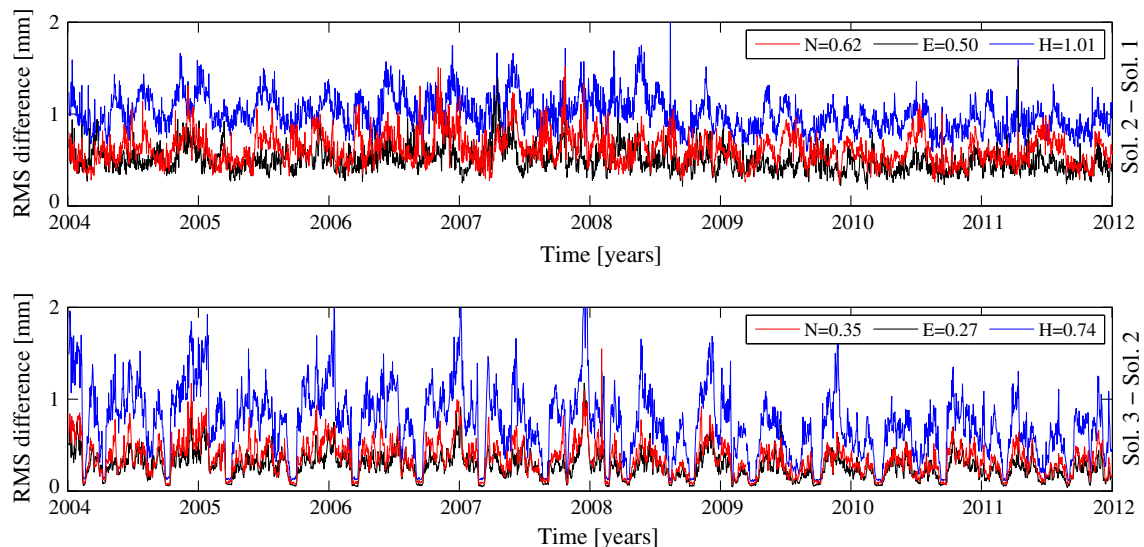
Fig. 9 RMS of differences of daily station coordinates (between one solution and the previous one, Helmert transformation not applied) over all available stations. The mean RMS values (mm) for the 8-year period are given in the upper right corner of the plots for each component

References

Amiri-Simkooei AR (2007) Least-squares variance component estimation: theory and GPS applications. PhD thesis, Delf University of Technology, Publications on Geodesy 64, Netherlands Geodetic Commission, http://www.ncg.knaw.nl/Publicaties/Geodesy/pdf/64AmiriSimkooei

Amiri-Simkooei AR (2013) On the nature of GPS draconitic year periodic pattern in multivariate position time series. J Geophys Res 118(5):2500–2511. doi:10.1002/jgrb.50199

Bar-Sever YE (1996) A new model for GPS yaw attitude. J Geod 70(11):714–723. doi:10.1007/BF00867149

Bar-Sever Y, Kuang D (2004) New empirically derived solar radiation pressure model for GPS Satellites. In: Interplanetary Network Progress Report, vol 42–159, http://ipnpr.jpl.nasa.gov/progress_report/42-159/title.htm

Beutler G, Brockmann E, Gurtner W, Hugentobler U, Mervart L, Rothacher M, Verdun A (1994) Extended orbit modeling techniques at the CODE processing center of the International GPS Service for Geodynamics (IGS): theory and initial results. Manuscr Geod 19(6):367–386

Bizouard C, Gambis D (2009) The Combined Solution C04 for Earth Orientation Parameters Consistent with International Reference Frame 2005. In: Drewes H (ed) Geodetic Reference Frames, IAG Symposia 134, Springer, pp 265–270, doi:10.1007/978-3-642-00860-3_41

Collilieux X, Altamimi Z, Coulot D, Ray J, Sillard P (2007) Comparison of very long baseline interferometry, GPS, and satellite laser ranging height residuals from ITRF2005 using spectral and correlation methods. J Geophys Res 112(B12403). doi:10.1029/2007JB004933

Dach R, Hugentobler U, Fridez P, Meindl M (2007) Bernese GPS Software, Version 5.0. Astronomical Institute, University of Bern

Dach R, Brockmann E, Schaer S, Beutler G, Meindl M, Prange L, Bock H, Jäggi A, Ostini L (2009) GNSS processing at CODE: status report. J Geod 83(3–4):353–365. doi:10.1007/s00190-008-0281-2

Dilssner F (2010) GPS IIF-1 satellite antenna phase center and attitude modeling. Inside GNSS 5(6):59–64

Dilssner F, Springer T, Gienger G, Dow J (2011) The GLONASS-M satellite yaw-attitude model. Adv Space Res 47(1):160–171. doi:10.1016/j.asr.2010.09.007

Dow JM, Neilan RE, Rizos C (2009) The International GNSS Service in a changing landscape of Global Navigation Satellite Systems. J Geod 83(3–4):191–198. doi:10.1007/s00190-008-0300-3

Fritsche M, Sosnica K, Rodriguez-Solano CJ, Steigenberger P, Wang K, Dietrich R, Dach R, Hugentobler U, Rothacher M (2014) Combined reprocessing of GPS, GLONASS and SLR Observations. J Geod, in press

Gobinddass ML, Willis P, de Viron O, Sibthorpe A, Zelensky NP, Ries JC, Ferland R, Bar-Sever Y, Diament M, Lemoine FG (2009) Improving DORIS geocenter time series using an empirical rescaling of solar radiation pressure models. Adv Space Res 44(11):1279–1287. doi:10.1016/j.asr.2009.08.004

Griffiths J, Ray JR (2013) Sub-daily alias and draconitic errors in the IGS orbits. GPS Solut 17(3):413–422. doi:10.1007/s10291-012-0289-1

Hugentobler U, van der Marel H, Springer T (2006) Identification and mitigation of GNSS errors. In: Springer T, Gendt G, Dow JM (eds) The International GNSS Service (IGS): perspectives and visions for 2010 and beyond, IGS Workshop 2006

King MA, Watson CS (2010) Long GPS coordinate time series: multipath and geometry effects. J Geophys Res 115(B04403). doi:10.1029/2009JB006543

Kouba J (2009) A simplified yaw-attitude model for eclipsing GPS satellites. GPS Solut 13(1):1–12. doi:10.1007/s10291-008-0092-1

Meindl M (2011) Combined analysis of observations from different global navigation satellite systems. PhD thesis, Astronomisches Institut der Universität Bern, Geodätisch-geophysikalische Arbeiten in der Schweiz, vol 83, http://www.sgc.ethz.ch/sgc-volumes/sgk-83

Meindl M, Beutler G, Thaller D, Dach R, Jäggi A (2013) Geocenter coordinates estimated from GNSS data as viewed by perturbartion theory. Adv Space Res 51(7):1047–1064. doi:10.1016/j.asr.2012.10.026

Ostini L (2012) Analysis and quality assessment of GNSS-derived parameter time series. PhD thesis, Astronomisches Institut der Universität Bern, http://www.bernese.unibe.ch/publist/2012/phd/diss_lo_4print.pdf

Press W, Teukolsky S, Vetterling W, Flannery B (1992) Numerical recipes in Fortran 77: the art of scientific computing, 2nd edn. Cambridge University Press, Cambridge, New York, Melbourne

Ratcliff JT, Gross RS (2013) Combinations of Earth orientation measurements: SPACE2011, COMB2011 and POLE2011. JPL Publication 13–5, Jet Propulsion Laboratory, California Institute of Technology, ftp://euler.jpl.nasa.gov/keof/combinations/2011/SpaceCombPole2011

Ray J, Altamimi Z, Collilieux X, van Dam T (2008) Anomalous harmonics in the spectra of GPS position estimates. GPS Solut 12(1):55–64. doi:10.1007/s10291-007-0067-7

Rebischung P, Altamimi Z, Springer T (2014) A collinearity diagnosis of the GNSS geocenter determination. J Geod 88(1):65–85. doi:10.1007/s00190-013-0669-5

Rodriguez-Solano CJ, Hugentobler U, Steigenberger P, Lutz S (2012a) Impact of Earth radiation pressure on GPS position estimates. J Geod 86(5):309–317. doi:10.1007/s00190-011-0517-4

Rodriguez-Solano CJ, Hugentobler U, Steigenberger P (2012b) Adjustable box-wing model for solar radiation pressure impacting GPS satellites. Adv Space Res 49(7):1113–1128. doi:10.1016/j.asr.2012.01.016

Rodriguez-Solano CJ, Hugentobler U, Steigenberger P, Allende-Alba G (2013) Improving the orbits of GPS block IIA satellites during eclipse seasons. Adv Space Res 52(8):1511–1529. doi:10.1016/j.asr.2013.07.013

Rothacher M, Beutler G, Herring TA, Weber R (1999) Estimation of nutation using the Global Positioning System. J Geophys Res 104(B3):4835–4859. doi:10.1029/1998JB900078

Santamaría-Gómez A, Bouin MN, Collilieux X, Wöppelmann G (2011) Correlated erros in GPS position time series: Implications for velocity estimates. J Geophys Res 116(B01405). doi:10.1029/2010JB007701

Seitz M, Angermann D, Bloßfeld M, Drewes H, Gerstl M (2012) The 2008 DGFI realization of the ITRS: DTRF2008. J Geod 86(12):1097–1123. doi:10.1007/s00190-012-0567-2

Sibthorpe A, Bertiger W, Desai SD, Haines B, Harvey N, Weiss JP (2011) An evaluation of solar radiation pressure strategies for the GPS constellation. J Geod 85(8):505–517. doi:10.1007/s00190-011-0450-6

Tregoning P, Watson C (2009) Atmospheric effects and spurious signals in GPS analysis. J Geophys Res 114(B09403). doi:10.1029/2009JB006344

Tregoning P, Watson C (2011) Correction to "Atmospheric effects and spurious signals in GPS analysis". J Geophys Res 116(B02412). doi:10.1029/2010JB008157

Wu X, Ray J, van Dam T (2012) Geocenter motion and its geodetic and geophysical implications. J Geodyn 58:44–61. doi:10.1016/j.jog.2012.01.007

Zumberge JF, Heflin MB, Jefferson DC, Watkins MM, Webb FH (1997) Precise point positioning for the effcient and robust analysis of GPS data from large networks. J Geophys Res 102(B3):5005–5017. doi:10.1029/96JB03860